Electronic Supplementary Material (ESI) for Chemical Communications.

Supporting Information

Synthesis and Characterisation of N-gene targeted NIR-II Fluorescent Probe for Selective Localisation of SARS-CoV-2

Parikshit Moitra,[a] Maha Alafeef,[a,b,c,d] Ketan Dighe,[a,b] Zach Sheffield,[b] Dipendra Dahal,[a] Dipanjan Pan*[,a,b,c,e]

[a] Center for Blood Oxygen Transport and Hemostasis, Department of Pediatrics, University of Maryland Baltimore School of Medicine, 670 W Baltimore St., Baltimore, Maryland 21201, USA

[b] Department of Chemical, Biochemical and Environmental Engineering, University of Maryland Baltimore County, 1000 Hiltop Circle, Baltimore, Maryland 21250, USA

[c] Bioengineering Department, University of Illinois at Urbana-Champaign, Illinois 61801, USA

[d] Biomedical Engineering Department, Jordan University of Science and Technology, Irbid 22110, Jordan

[e] Department of Diagnostic Radiology and Nuclear Medicine, University of Maryland Baltimore, 670 West Baltimore Street, Baltimore, Maryland 21201, United States

*Correspondence: dipanjan@som.umaryland.edu

Table of contents **Page No.**

Figures.

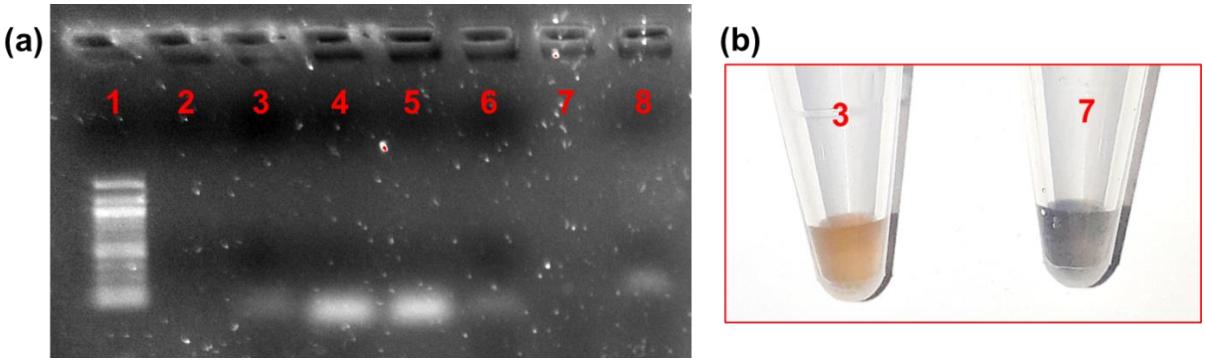

Figure S1. (a) Agarose gel electrophoresis to prove the covalent attachment of ASO to the PbS QD nanoparticle. Lane 1: 100 bp DNA ladder; lane 2: oleic acid capped QD; QD-ASO nanoparticle alone (lane 3) and treated with β-mercaptoethanol (lane 4), dithiothreitol, DTT (lane 5), tris(2-carboxyethyl)phosphine hydrochloride, TCEP (lane 6), sodium borohydride, $NaBH_4$ (lane 7) and lysis buffer having high salt concentration (lane 8). (b) Photographic images of QD-ASO nanoparticle before and after the addition of sodium borohydride.

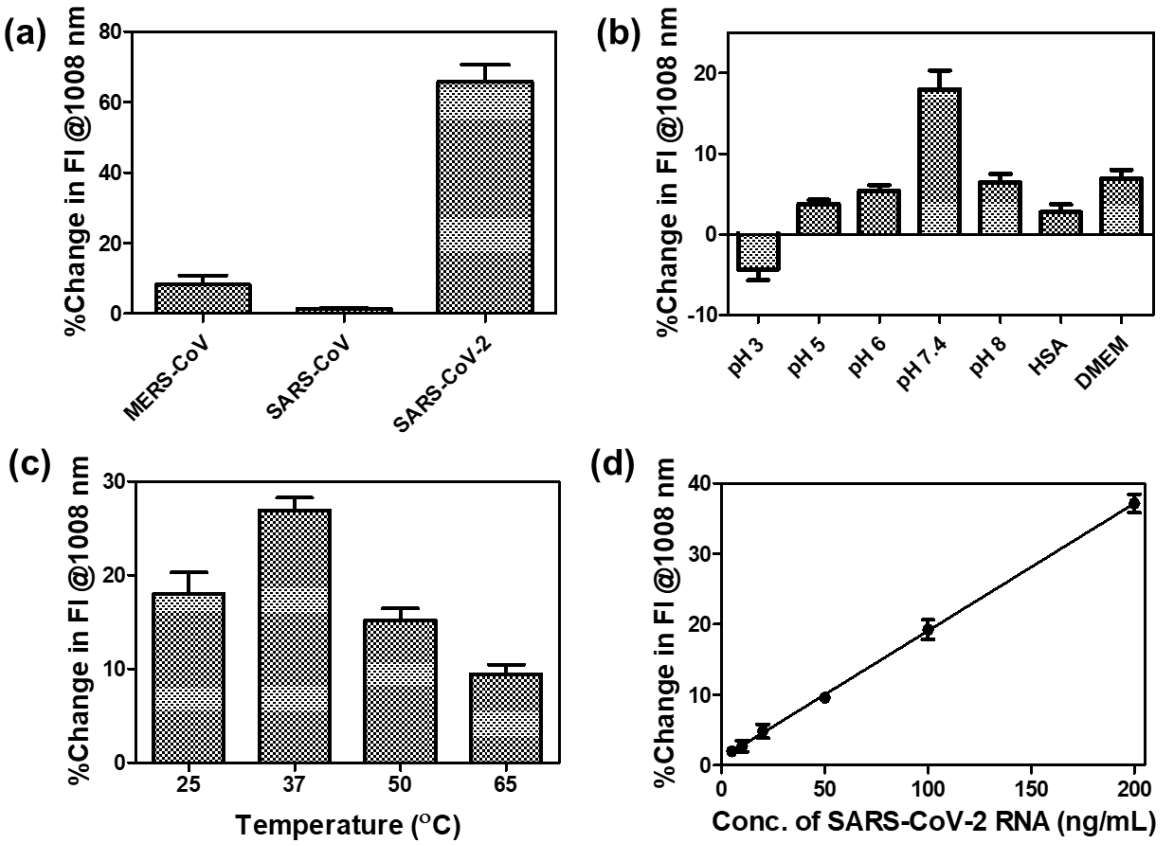

Figure S2. (a) Change in emission of QD-ASO suspension at 1008 nm when MERS-CoV, SARS-CoV and SARS-CoV-2 viral RNA were added at a concentration of 5 ng/µL. (b) Change in fluorescence of QD-ASO with SARS-CoV-2 RNA (1 ng/µL) with the change in pH of the medium (3, 5, 6, 7.4 and 8), presence of HSA (0.5 mg/mL) and complex suspension like cell culture media, DMEM. (c) Change in emission of QD-ASO nanoparticle with the change in temperature and (d) Calculation of limit of detection of QD-ASO nanoparticle for SARS-CoV-2 RNA.

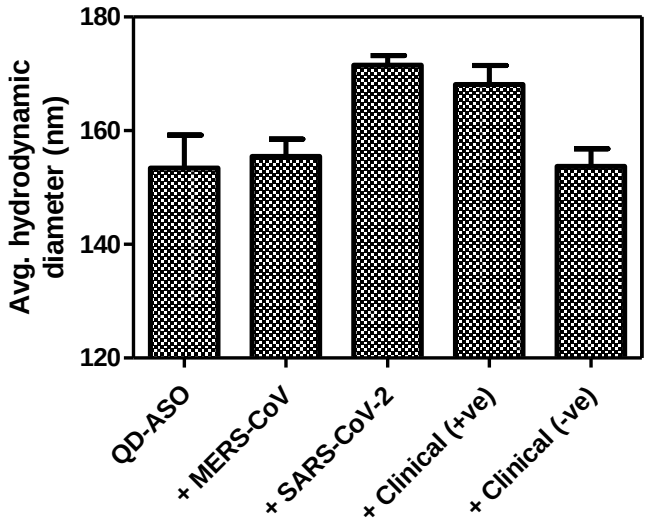

Figure S3. Average hydrodynamic diameter of ASO conjugated PbS-QD in absence and presence of MERS-CoV and SARS-CoV-2 RNA. The change in hydrodynamic diameter in presence of SARS-CoV-2 positive and negative clinical samples are also presented.

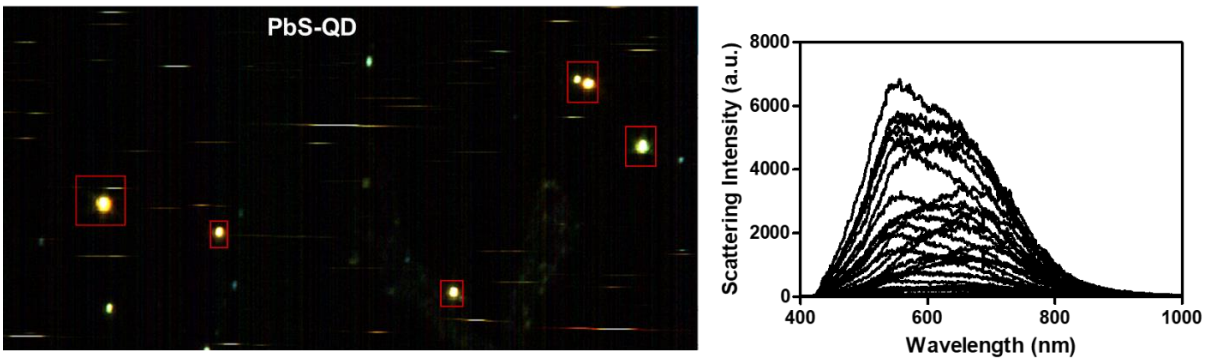

Figure S4. EDFM-HSI of oleic acid capped PbS QD has been shown at the left. The hyperspectral data as obtained from multiple positions of the image has been represented at the right.

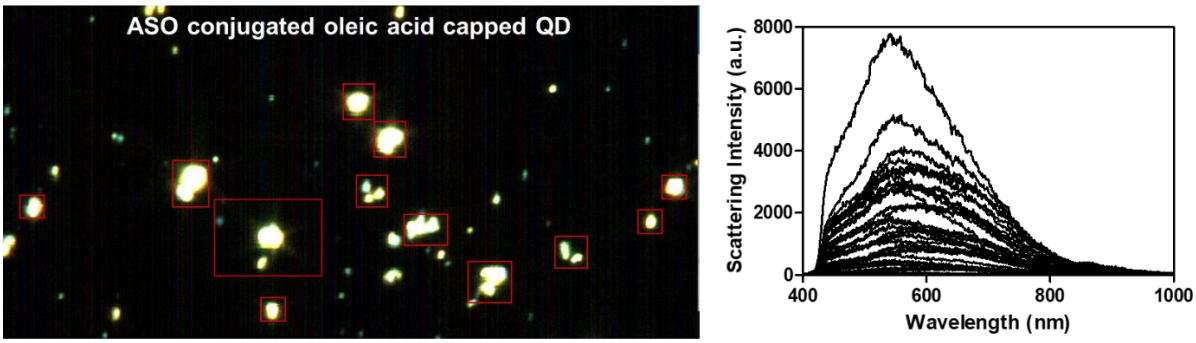

Figure S5. EDFM-HSI of QD-ASO has been shown at the left. The hyperspectral data as obtained from multiple positions of the image has been represented at the right.

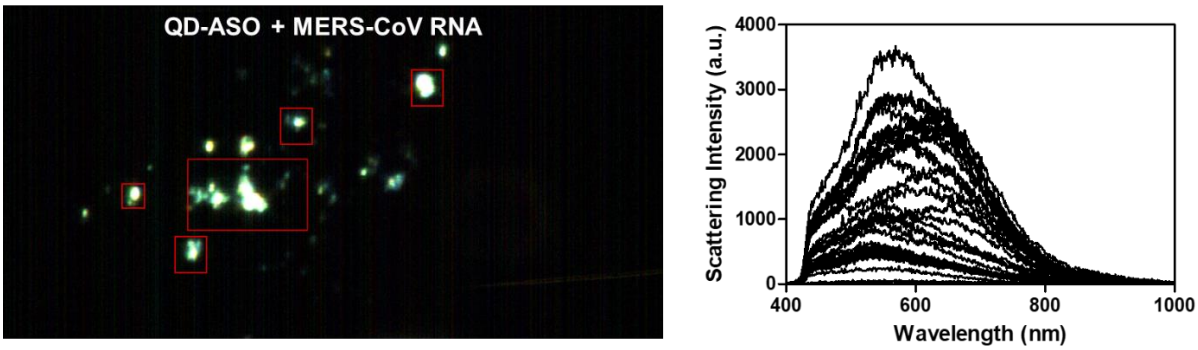

Figure S6. EDFM-HSI of QD-ASO in hybridisation with viral MERS-CoV RNA has been shown at the left. The hyperspectral data as obtained from multiple positions of the image has been represented at the right.

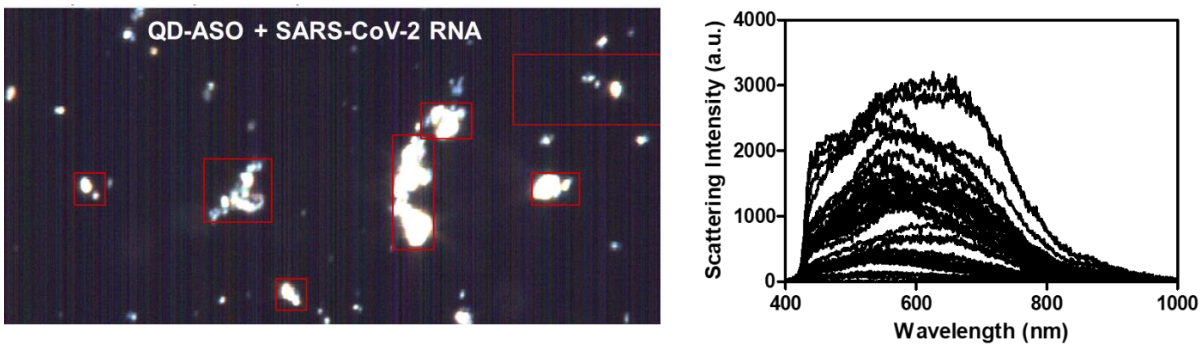

Figure S7. EDFM-HSI of QD-ASO in hybridisation with viral SARS-CoV-2 RNA has been shown at the left. The hyperspectral data as obtained from multiple positions of the image has been represented at the right.

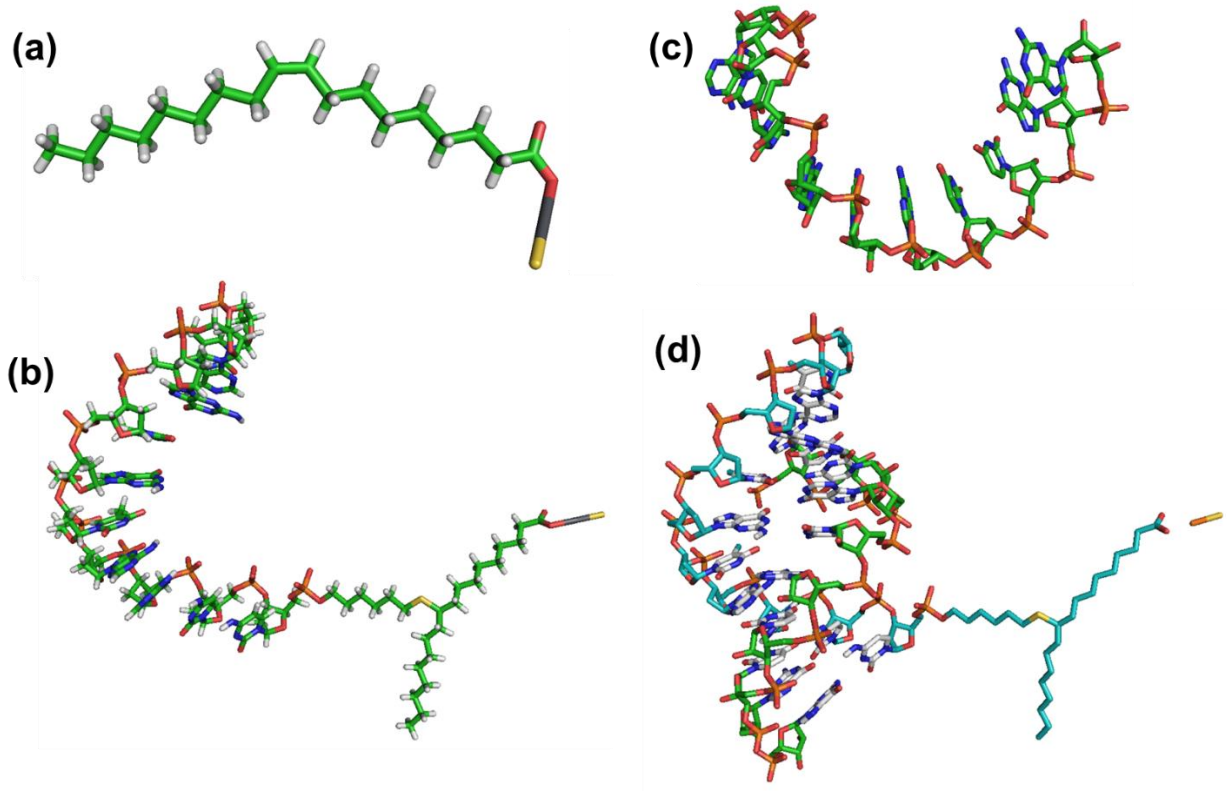

Figure S8. B3LYP/ 6-31G(d) energy minimised structures of (a) oleic acid capped lead sulfide quantum dot (PbS-QD); (b) ASO conjugated PbS-QD (QD-ASO); (c) target

segment of SARS-CoV-2 RNA and (d) hybridised geometry of QD-ASO and SARS-CoV-2 RNA (QD-ASO-RNA).

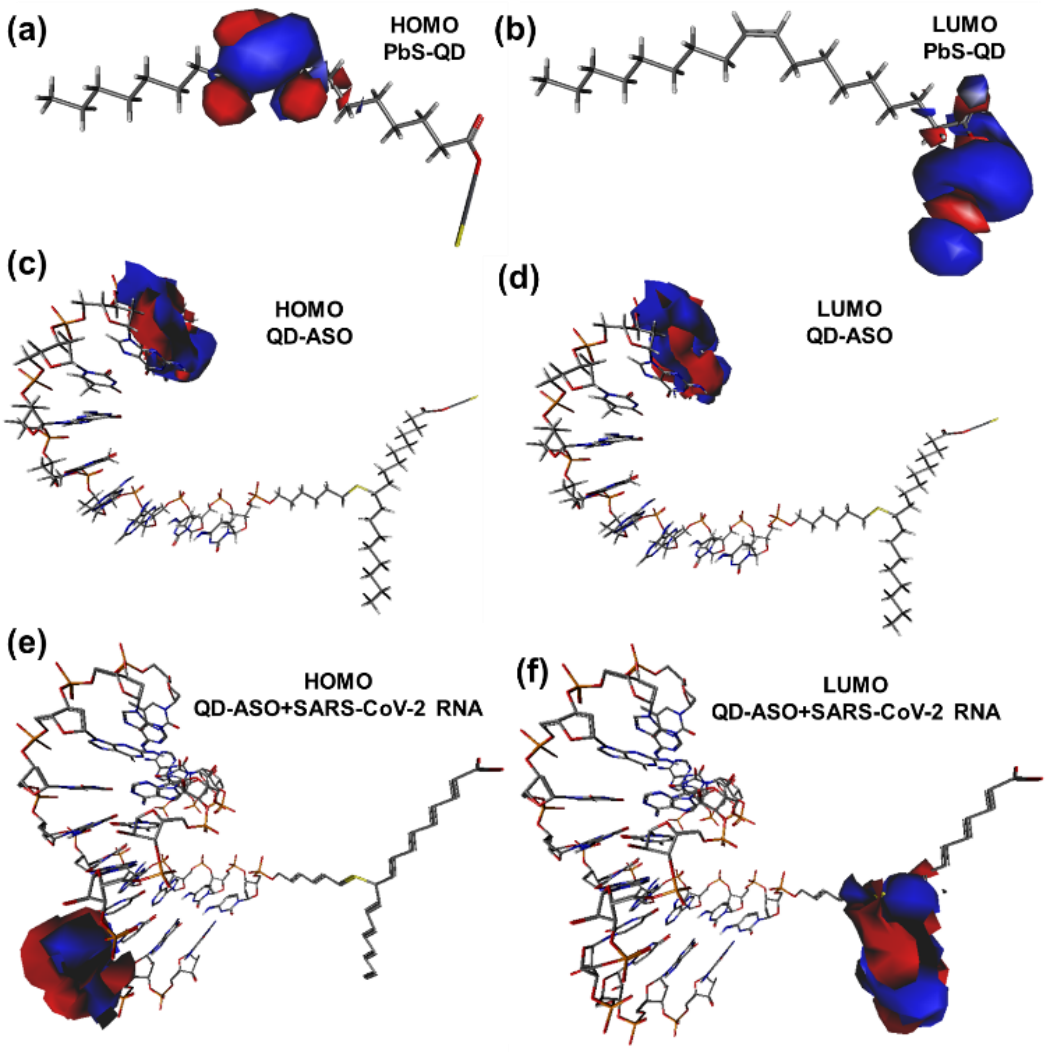

Figure S9. Pictorial representations of (a, c, e) HOMO and (b, d, f) LUMO energy orbitals for (a, b) PbS-QD; (c, d) QD-ASO and (e, f) RNA hybridised with QD-ASO.

Table S1. Comparison of HOMO-LUMO energy gap among oleic acid capped PbS QD and ASO conjugated QD before and after its hybridisation with SARS-CoV-2 RNA.

Compound	$\Delta E_{HOMO-LUMO}$ in Hartee	$\Delta E_{HOMO-LUMO}$ in eV
PbS-QD	0.036	0.97
QD-ASO	0.0419	1.14
QD-ASO-RNA	0.0056	0.15

Materials and Methods.

Materials. The thiol modified antisense oligonucleotide (ASO) was procured from Sigma and stored at −20 °C. Oleic acid capped NIR-II active lead sulfide quantum dots (PbS-QD), suspended in toluene, were acquired from Strem Chemicals (Catalog number 82-1081) and used as obtained. Purified RNA extraction kit was purchased from Invitrogen. All the other chemicals were purchased from reputable commercial vendors and used without any further purification. All the experiments were carried out at constant room temperature of 25 °C.

Functionalisation of ASO. 200 µL of PbS-QD was taken from a stock concentration of 10 mg/mL and diluted to a final volume of 2 mL in a quartz cuvette with toluene. 10 µL of ASO was then added to the solution from a stock of 200 µM in TE buffer. This was followed by the addition of 100 µL of a 10 mg/mL solution of dimethoxy phenylacetatone (DMPA). The suspension was mixed adequately and placed inside Tri-Light UV irradiator. The suspension was irradiated with UV light for 5 mins. The cuvette was removed from the reaction chamber and cooled to room temperature by placing it on ice. Methanol was

then added to the suspension dropwise (about 100 µL) until the mixture appears homogenous. The cuvette was placed back inside the chamber and further irradiated for 10 minutes and then cooled on ice. This process was repeated for three additional times. Finally, the suspension was centrifuged at 10,000 rcf for 15 minutes, supernatant discarded, washed with toluene and centrifuged again to obtain the pellet. The residue was redispersed again in chloroform and centrifuged to obtain the pellet. This step with chloroform was repeated twice to remove any unexpected reactant residues from the conjugation step. The obtained residue was further redispersed in ethanol, centrifuged and dried in vacuum to obtain the dry pellet. This is finally suspended in required volume of RNAse free water to obtain an intended concentration of nanoparticles.

^{1}H NMR spectroscopy. The ^{1}H NMR spectra were recorded on a Bruker 600 MHz spectrometer.

Calculation of %ASO conjugation. The peak at 1.10 ppm for QD-ASO nanoparticle (Figure 1b in the main manuscript) corresponds to oleic acid protons where no other nucleotide protons would interfere. From the chemical structure of oleic acid, it can be said that there should be 25 protons at 1.10 ppm. Accordingly, the peak from 7.39-8.42 ppm can be correlated with the aromatic protons of nucleotide. It has been calculated from the ASO structure (sequence: CCAATGTGATCTTTTGGTGT) having 20 nucleotide base pair that there should be 23 protons in this region.

Now, by comparing and calibrating the integration of the NMR spectra for the aromatic protons with respect to the oleic acid protons, it was observed that there are only 12.6 protons instead of 23. Hence, the %conjugation can be calculated as (12.6/23)

*100 = 54.8%. This means that there are 54.8 number of ASOs bonded to each 100 molecules of oleic acid capped on the surface of QD.

Gel Electrophoresis. 1% agarose gel was prepared in 0.5x TBE buffer and run on 100V for 45 mins. 100 bp DNA ladder; oleic acid capped QD; QD-ASO nanoparticle alone and treated with β-mercaptoethanol, dithiothreitol (DTT), tris(2-carboxyethyl)phosphine hydrochloride (TCEP), sodium borohydride ($NaBH_4$) and lysis buffer having high salt concentration were run at different lanes. The gel was finally stained with 3x Gelred dye and imaged with Biorad GelDoc. The lysis buffer solution (Invitrogen catalog number 15577018) was used at 1/20 dilution where the final concentration of guanidine isothiocyanate, Tris-HCl (pH 7.5) and EDTA was 200 mM, 2.5 mM and 1.25 mM respectively.

Isolation of RNA. The total RNA was extracted and purified from the BEI obtained cellular lysate with a commercially available RNA purification kit following manufacturers' protocol. The concentration of purified total RNA as extracted from Vero cell lysate infected with SARS-CoV-2 was determined by ThermoScientific Nanodrop and it was found to be 35.9 ng/µL.

The clinical samples tested in this work were collected as part of the registered protocols approved by the Institutional Review Board (IRB) of the University of Maryland, Baltimore. The nasopharyngeal swab samples (clinically identified COVID +ve and -ve) were stored in viral transfer media and stored at -80 °C for future use.

UV-Visible absorbance spectra. The absorbance spectra were recorded on a VWR UV–vis spectrophotometer.

Fluorescence spectra. The fluorescence emission spectra of QD-ASO nanoparticles were recorded on a Horiba Fluoromax plus spectrophotometer at an excitation wavelength of 750 nm. The emission spectra were recorded from 760-1150 nm with excitation and emission slit width of 5 nm each. The probe found to have an emission maximum at 1008 nm when excited at 750 nm.

Measurement of size and zeta potential. The average hydrodynamic diameter and zeta potential of the nanoparticles before and after the addition of RNA were monitored on a particle tracking analyser (Zetaview Particle Metrix). The particles were diluted to an optimum extent before each measurement and multiplied by the dilution factor to obtain the results. The machine chamber was properly cleaned prior each measurement.

Transmission electron microscopy. A 20 µL solution of the nanoparticles before and after the addition of RNA was added on top of a carbon-coated copper grid (400 mesh). This was allowed to stay for about 10 minutes before being removed with a filter paper and imaged under a transmission electron microscope (FEI tecnai T12). The tungsten filament with 80 kV accelerating voltage was used for the investigations.

Hyperspectral analyses. A 20 µL suspension of nanoparticles before and after the addition of RNA was drop casted on top of a glass slide and covered with a cover slip immediately. The slides were air-dried prior measurements and imaged with a enhanced dark-field optical microscope (Cytoviva). The hyperspectra were acquired using the hyperspectral recorder from Cytoviva. Based on the hyperspectral data set, the spectrum of scattering at each pixel was obtained using the CytoViva software program (ENVI 4.8). For collecting the representative hyperspectrum, hyperspectral scattering signals were

collected from various spatial locations of the captured image. The collected spectra were then averaged to obtain the representative signal for each sample.

Energy Minimisation and docking studies. The chemical structures of PbS-QD, QD-ASO and target RNA were first energy optimised using a general ab initio quantum chemistry package, General Atomic and Molecular Electronic Structure System (GAMESS) program. The target RNA strand sequence is 5'-AUCACAUUGG-3', whereas the ASO sequence is 5'-HS-C_6-CCAATGTGAT-3'. MINI functional was used as the Huzinaga's 3 gaussian minimal basis set with Pople N31 for the polar groups while performing the density functional theoretical (DFT) calculations. The energies minimised structures of target RNA and QD-ASO were then undertaken for docking studies using AutoDock 4.0 software.

HOMO-LUMO calculations. The energy minimised structures and the most stable docked geometry were then used for HOMO-LUMO energy orbital calculations using GAMESS program as described above. The highest occupied molecular orbital energy (E_{HOMO}), the lowest unoccupied molecular orbital energy (E_{LUMO}) and the energy gap between E_{LUMO} and E_{HOMO} was calculated and represented as $\Delta E_{LUMO\text{-}HOMO}$.

NIR-II microscope imaging. The lung tissue sections were obtained from a sacrificed BALB/c mouse and injected with clinically positive SARS-CoV-2 RNA on its top surface. After 15 mins, 20 µL of QD-ASO nanoparticles were injected on the top surface of the tissue section and incubated for 30 mins at room temperature. The tissue sections were then imaged under Nikon Ti2-E Inverted Automated Research Microscope. NIRvana 640ST camera was used for NIR-II imaging and pco.edge 4.2bi back illuminated cooled sCMOS camera was used for bright field and Cy5 fluorescent channel imaging.

CY5/Alexa Fluor 647/Draq 5 filter set, excitation: 620/50nm (595-645nm), emission: 690/50nm (665-715nm), dichroic mirror: 655nm was used for Cy5 fluorescence channel. ET850/40x Chroma ET Series excitation filter and ET1000/100m Chroma ET Series emission filter with custom 50/50 beam splitter was used for NIR-II microscopic imaging.